Journal of Imaging Science and Technology® 51(6): 540–546, 2007.

The Latent Image Formation Process of Silver Salt Photothermographic Materials: Photoconductivity Decay Kinetics in Silver Halide Crystals with Silver Carboxylate

Soc Man Ho Kimura, Tetsuya Suzuki and Tsuyoshi Mitsuhashi
R&D Center, Konica Minolta Medical & Graphic, Inc., 1 Sakuramachi, Hino, Tokyo 191-8511, Japan
E-mail: socman.kimura@konicaminolta.jp

Ken'ichi Kuge▲ and Akira Hasegawa▲
Department of Information & Image Science, Faculty of Engineering, Chiba University, 1-33 Yayoicho, Inage, Chiba 263-8522, Japan

Abstract. *In exploring the latent image formation mechanism of silver salt photothermographic materials, we measured the microwave photoconductivity of nanometer-scale silver halide crystal emulsions under optimal conditions and thereby observed the influence of silver carboxylate on those emulsions. We found that as the concentration of silver carboxylate increased, so did the number of shallow electron traps. In addition, when silver carboxylate was present, the lifetime of excited electrons showed quick decay. These observations suggest that silver carboxylate greatly affects latent image formation in silver salt photothermographic materials. © 2007 Society for Imaging Science and Technology.*
[DOI: 10.2352/J.ImagingSci.Technol.(2007)51:6(540)]

INTRODUCTION

Background

Conventional silver halide photographic materials (wet films) employ a liquid developer, while silver salt photothermographic materials (dry films) are developed using heat and without liquid processing. However, in both cases latent image centers are generated when silver halide crystals absorb light upon exposure.

The well-known latent image formation mechanism in wet film may be thought of as a "step-by-step mechanism." Silver halide crystals absorb light to generate photoelectrons and holes. Electron traps then trap photoelectrons, and the trapped photoelectrons subsequently attract and react with interstitial silver ions, thus forming silver atoms. The repetition of this cycle of electronic and ionic processes at a given location results in a cluster of silver atoms that constitute a latent image center. The totality of such latent image centers constitutes the latent image.

On the other hand, Cowdery–Corvan and Whitcomb recently compiled much information on the latent image formation mechanism of dry film.[1] Whether the latent image formation process of dry film is the same as that of wet film has been addressed by many hypotheses. For example, Zou et al. reported that the heterojunction between a silver carboxylate crystal and a silver halide crystal functions as an electron trap, so that silver ions move directly from the silver carboxylate crystal to the silver halide crystal.[2(a)] They suggested that contact between the silver carboxylate crystals and the silver halide crystals is critical. On the other hand, Strijckers et al., using a transmission electron microscope, observed a developing starting point and reported that developing silver is formed even when there is no contact between the silver carboxylate crystals and the silver halide crystals.[3] Furthermore, Yamane et al., upon examining the relationship between silver halide crystal dimensions and photographic sensitivity in dry film, reported that photographic sensitivity is proportional to silver halide crystal volume, and concluded that the latent image formation mechanism of dry film is identical to that of wet film.[4]

No well-defined mechanism of latent image formation has thus been advanced in the case of dry film. Various discussions[2–4] of the latent image formation mechanism involved with dry film have focused on the photographic sensitivity and observation after high temperature development process by transmission electron microscope. This literature has lacked discussion of the behavior of photoelectrons in the nanometer-scale silver halide crystals.

A characteristic of commercial dry film that is different from wet film is that silver halide crystals of nanometer-scale are used in the imaging layer in both "organic solvent-based photothermographic materials" and "water-based photothermographic materials." In addition, in the dry films silver halide crystals are surrounded by a large quantity of silver carboxylate, which supplies the silver for image formation. It is thought that this environment may have some influence on the latent image formation, and thereby make latent image formation different in dry film when compared to wet film.

Experimental Strategy

We investigated the latent image formation mechanism of dry film via microwave photoconductivity. We paid particu-

▲IS&T Members

Received Mar. 24, 2007; accepted for publication Jul. 18, 2007.
1062-3701/2007/51(6)/540/7/$20.00.

lar attention to the use, in dry film, of nanometer-scale silver halide crystals surrounded by a large quantity of silver carboxylate. To simplify the systems involved, we prepared the admixtures of nanometer-scale silver halide crystal emulsions and silver carboxylates in the gelatin/water medium. There were no photographic additives, and we did not deliberately make an epitaxial interface between the silver carboxylate and silver halide crystals. We mixed silver halide emulsion and silver carboxylate liquid dispersion just before coating. Then we measured the microwave photoconductivity for coating samples of the admixtures.

No previous microwave photoconductivity measurement of nanometer-scale silver halide crystals had been reported, and, due to their relatively low sensitivity to light, we anticipated difficulty detecting a microwave photoconductivity signal with nanometer-scale crystals. It was therefore unclear what conditions were best for measuring the photoconductivity of such small crystals, and those conditions had to first be determined. To accomplish this, we measured microwave photoconductivity at varying degrees of silver coverage and measurement wavelengths. We found an optimal range of silver coverage, allowing us to obtain a photoconductivity signal of ample strength.

Having determined optimal measurement conditions, we measured the photoconductivity of the admixture samples of nanometer-scale silver halide crystals and silver carboxylate at different ratios. Under our measurement conditions, we obtained data regarding photoconductivity decay kinetics, data whose analysis provided new insights into the latent image formation mechanism of dry film.

EXPERIMENTAL

Preparation of AgBrI Crystal Emulsions

Nanometer-scale silver halide crystal emulsions were prepared containing cubic $AgBr_{0.98}I_{0.02}$ crystals produced by the double jet method. Seven emulsions were prepared, each of a different average crystal edge length and with the following crystal edge length distributions: 33 nm (12%), 35 nm (13%), 43 nm (10%), 80 nm (10%), 92 nm (13%), 124 nm (13%), and 148 nm (11%). All of the emulsions were at pAg 8.3 and none were spectrally or chemically sensitized.

Preparation of Powdery RCOOAg

Using fatty acids employed in commercial dry film, 250 g of fatty acids (45% behenic acid, 34% arachidic acid, and 21% stearic acid) were dissolved in 4720 ml water at 80°C, after which 540.2 ml of 1.5 M aqueous sodium hydroxide solution was added with vigorous stirring. Subsequently, 6.9 ml of concentrated nitric acid was added to adjust the pH value from 10 to 9. The obtained solution of aqueous fatty acid sodium salts was cooled to 55°C, after which 760.6 ml of 1 M aqueous silver nitrate solution was added over less than two minutes, and the mixture was stirred for more than 20 minutes. The reaction mixture was then filtered to remove water soluble salts. Thereafter, washing with deionized water and filtration were repeated until the filtrate reached a conductivity of 2 μS/cm. After spin-drying by centrifuge, the reaction product was further dried with heated air until there was no reduction in weight. In this way, powdery RCOOAg was obtained.[4]

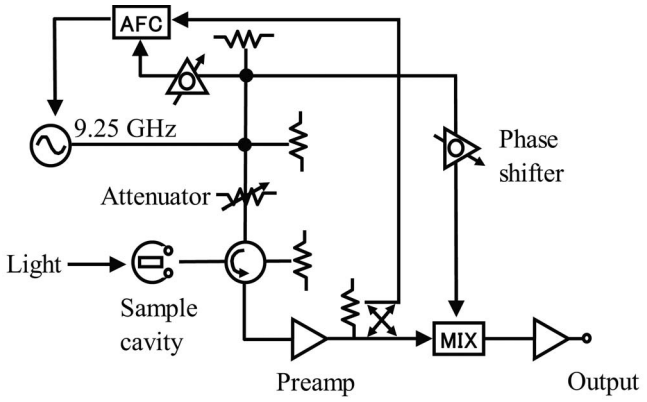

Figure 1. Microwave photoconductivity measuring apparatus.

Preparation of RCOOAg-AgBrI Admixtures

Because the emulsions in the following admixtures differ from emulsions found in commercial dry film, the admixtures are referred to hereafter as "RCOOAg-AgBrI admixtures." To prepare a simple system with no epitaxial interface between the silver carboxylate crystals and the silver halide crystals, the powdery silver carboxylate was added to a 5 wt% phenylcarbamoyl gelatin solution without any surfactants while stirring. The mixture was then subjected to ultrasonic dispersion for three hours in an ice bath. The resultant gelatin solution containing dispersed silver carboxylate was then mixed, in a range of ratios, with each of the seven silver halide crystal emulsions of differing crystal edge length previously described. To prevent the generation of in situ AgBr, no antifoggant (such as zinc bromide or calcium bromide) was added. Similarly, to prevent the formation of mobile silver ion complexes, which would obstruct observation of the reactions generating silver clusters, no silver ion complexing agent, toner agent, or silver ion carrier (such as phthalazine or tetrachlorophthalic acid) was added.

Measurement of Microwave Photoconductivity

To measure microwave photoconductivity, we employed a homodyne method with a 9.25 GHz Gunn oscillator (Figure 1).[5] The light source was a Nd:YAG pulsed laser beam (wavelength, 355 nm; pulse width, 3 ns; light energy, 0.02 to 0.2 J/m^2) filtered by two color filters with transmissions at 420 nm and 440 nm, respectively. The measurement temperature was 22°C.

Analysis of Microwave Photoconductivity

A transient photoconductivity decay signal typical of silver halide is shown in Figure 2(a). The signal can be ascribed almost completely to free electrons. From this fact and from reports of such responses,[6–8] we identified two components of decay [Fig. 2(b)]. Signal intensity (I) is proportional to the number of free electrons in the conduction band when electron trapping and thermal detrapping equilibrate imme-

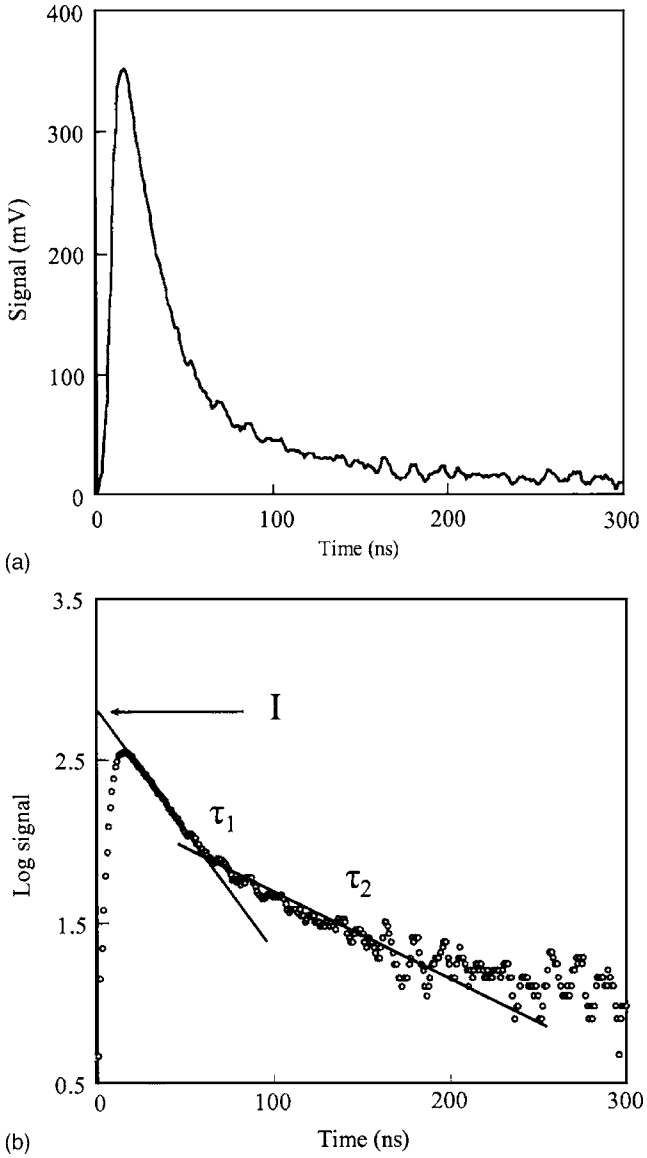

Figure 2. (a) A typical signal encountered in microwave photoconductivity measurement. (b) Logarithmic plot of data from (a), showing the two components (τ_1, τ_2) of decay. Signal intensity (I) is inferred from initial signal magnitude.

diately upon sample exposure. The faster component of decay (τ_1) indicates the transit of electrons from shallow to deeper electron traps as the result of a lattice relaxation. The slower component of decay (τ_2) indicates trapped electrons reacting with mobile silver ions. These data allowed us to distinguish between decay ascribable to electronic processes and decay ascribable to ionic processes.

RESULTS

Measurement of Microwave Photoconductivity of Nanometer-scale AgBrI Crystal Emulsions

We first measured the microwave photoconductivity of the nanometer-scale AgBrI emulsion samples with silver halide crystals of various edge lengths. We coated the emulsion on a colorless polyethylene terephthalate base with a silver coverage of 50 mg/dm^2. A 355 nm laser was used that provided

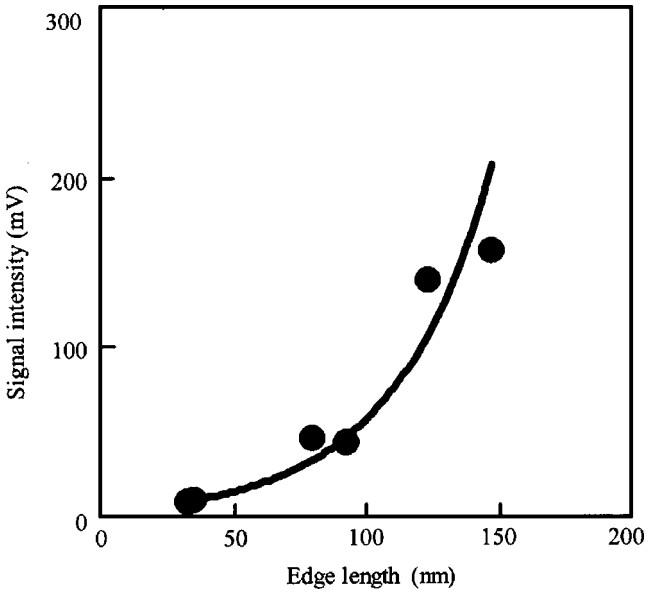

Figure 3. Relationship between microwave photoconductivity signal intensity and edge length of silver halide crystals in AgBrI emulsions.

0.05 J/m^2 of light energy. The relationship between signal intensity and edge length in Figure 3 shows that, as predicted, the microwave photoconductivity signals of the nanometer-scale crystals are weak. The commensurate reduction in signal-to-noise ratio makes microwave photoconductivity measurement difficult.

In search of a stronger signal, we measured the microwave photoconductivity of the AgBrI emulsion containing the smallest crystals (33 nm) at various degrees of silver coverage and with exposure to one of the three wavelengths of laser light. We achieved silver coverages exceeding 600 mg/dm^2 for the thickest emulsion coatings. Figure 4

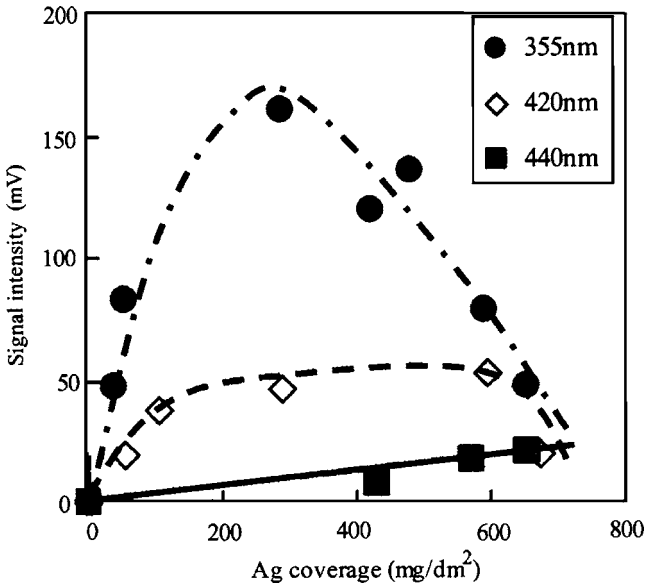

Figure 4. Silver coverage versus microwave photoconductivity signal intensity for 33 nm AgBrI crystal emulsions measured at wavelengths of 355, 420, 440 nm.

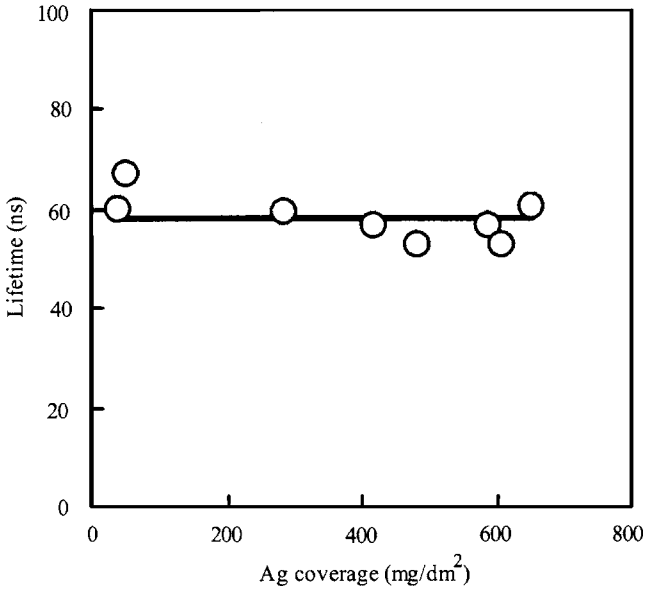

Figure 5. Photoelectron lifetimes from the 355 nm wavelength data in Fig. 4.

shows the dependence of signal intensity on silver coverage. The photoconductivity signal intensity (I) at a wavelength of 440 nm increases steadily but only gradually with increasing silver coverage. At 420 nm and 355 nm, however, signal intensity increases rapidly with silver coverage, reaches a maximum, and then decreases. This can be ascribed to the difficulty light of these wavelengths has reaching the interior of the sample, so that the light is no longer absorbed uniformly throughout the sample. In addition, the increase of silver coverage results in an increased loss of microwave electric power and in a lower cavity resonator quality factor.

We observed a similar relationship between silver coverage and signal intensity with our remaining nanometer-scale AgBrI emulsion samples. Similar results were reported by Kellogg et al.[9] with micrometer-scale crystals (0.5 μm, cubic $AgBr_{0.97}I_{0.03}$). It may be that this phenomenon appears with silver halide crystals of every magnitude.

Signal intensity increased when the wavelength of irradiating light was shortened from 440 nm to 420 nm to 355 nm. This may have been due to an increase in the light absorption of silver halide at the shorter wavelengths. These results indicate that the optimal condition for the measurement of microwave photoconductivity of 33 nm silver halide crystals is an irradiating light wavelength of 355 nm and a silver coverage of 200 mg/dm^2 or less. Under these conditions, we irradiated samples with a light energy exceeding 0.1 J/m^2. When exposed to light of wavelengths corresponding to the inherent sensitivity of nanometer-scale silver halide crystals, the decay of photoelectrons could be detected via microwave photoconductivity.

While a change in silver coverage resulted in a change in signal intensity, silver coverage had little effect on photoelectron lifetime, as shown in Figure 5. This is consistent with the generation and decay of photoelectrons proceeding independently on each silver halide crystal.

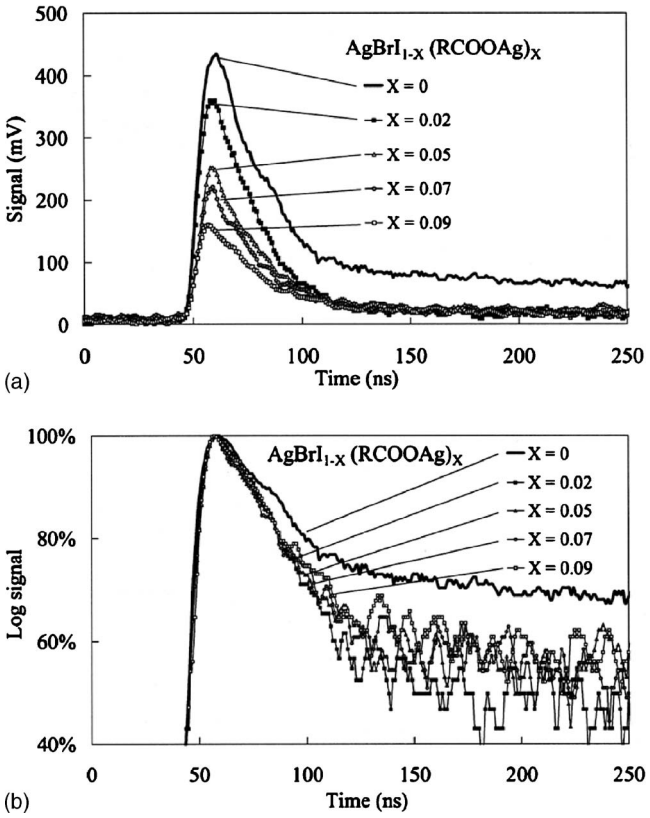

Figure 6. (a) Signals of microwave photoconductivity measurement, (b) normalized logarithmic plot of data from (a), showing the lifetime of electrons.

After establishing the optimal condition of microwave photoconductivity for the nanometer-scale crystals, we measured the photoconductivities of the RCOOAg-AgBrI admixtures. To obtain accurate measurement, we used the RCOOAg-AgBrI admixtures with 43 nm edge length crystals and a silver coverage of 100 mg/dm^2. Exposure was with laser light at a wavelength of 355 nm and a light energy of 0.2 J/m^2.

However, the thicknesses of the samples increased with the ratio of silver carboxylate, and this caused a decrease in signal intensity. We therefore used a ratio of silver carboxylate below 10 mol% at 100 mg/dm^2 of silver coverage from silver halide crystals to measure the microwave photoconductivity of the RCOOAg-AgBrI admixtures.

Measurement of Microwave Photoconductivity With RCOOAg-AgBrI Admixtures After One Exposure

The signal intensities of the microwave photoconductivity measurements with RCOOAg-AgBrI admixtures at differing ratios are shown in Figure 6(a). Normalized logarithmic plotting of intensity decay is shown in Fig. 6(b). Photoelectron lifetime was very short with the nanometer-scale silver halide crystals, and a great deal of noise was found in the latter half of the signal curve. This made it difficult to identify the second component in the decay curves in Fig. 6(b), although the decay curve for photoelectrons generally exhibits two components of photoelectron lifetime, as mentioned earlier. Consequently, we used only the slope of the first half of the signal curve in determining photoelectron lifetime.

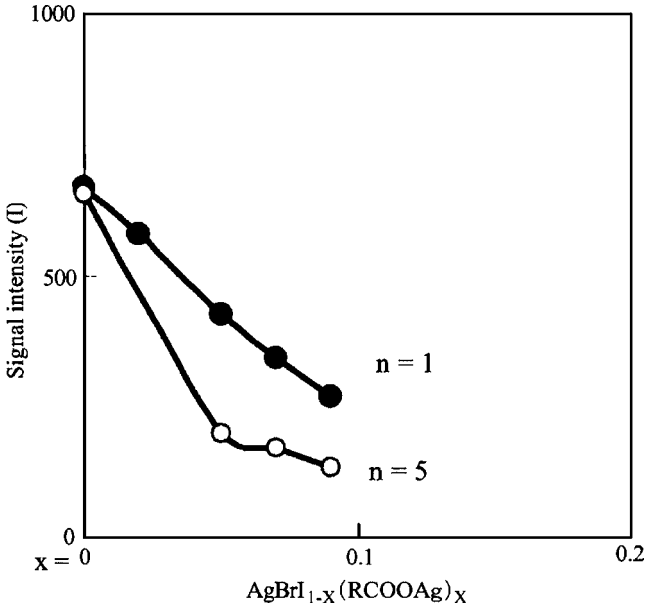

Figure 7. Signal intensity (I) of microwave photoconductivity of $AgBrI_{1-X}(RCOOAg)_X$ samples. Numerals (n) indicate the number of exposures to laser light.

In addition, the signal intensity of decay curve for all RCOOAg-AgBrI admixtures decayed to about 20 mV, whereas for pure silver halide emulsion the curve decayed to about 60 mV [Fig. 6(a)].

After a single exposure (Figure 7, $n=1$), signal intensity decreased in inverse correlation to an increase in the ratio of silver carboxylate, indicating that the number of free electrons decreases as silver carboxylate content increases. Similarly, after a single exposure (Figure 8, $n=1$), the introduction of silver carboxylate resulted in photoelectron lifetimes shorter than those obtained with the pure silver halide emulsion (although without correlation with the ratio of silver carboxylate present).

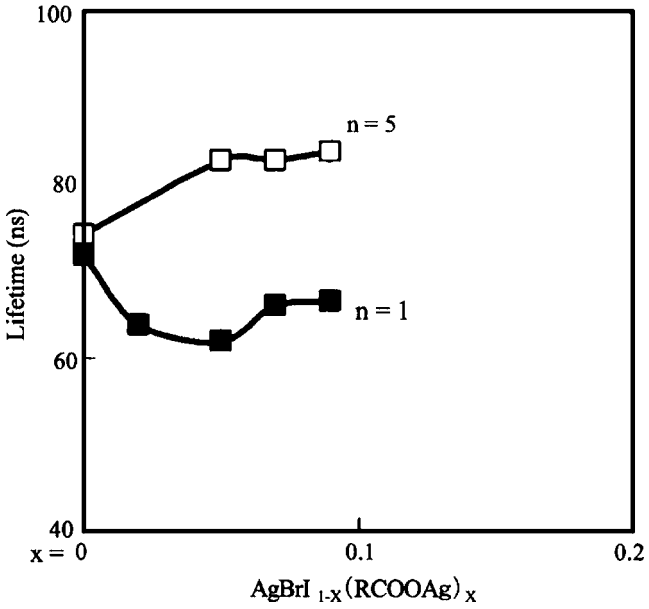

Figure 8. Photoelectron lifetimes of samples in Fig. 7. Numerals (n) indicate the number of exposures to laser light.

Measurement of Microwave Photoconductivity in RCOOAg-AgBrI Admixtures After Repeated Exposures

After five exposures (Fig. 7, $n=5$), signal intensity decreased with the ratio of silver carboxylate present, much as it did after single exposures. But where repeated exposure of the pure silver halide crystal emulsion brought only a marginal decrease in signal intensity, repeated exposure of samples across a range of silver carboxylate ratios resulted in substantial drops in signal intensity. Similarly, after five exposures (Figure 8, $n=5$), the introduction of silver carboxylate resulted in photoelectron lifetimes longer than obtained with the pure silver halide emulsion (although again without correlation with the ratio of silver carboxylate present).

DISCUSSION

Photoelectron Decay and Latent Image Formation

The nature of the transition responsible for the photoconductivity transient decay signal has yet to be clearly defined, but one way in which photoconductivity relates to latent image formation involves a lattice relaxation model.[8] In this model, silver halide crystals absorb light to generate photoelectrons (e_f) in the conduction band and holes (h) in the valence band:

$$h\upsilon \rightarrow e_f + h. \tag{1}$$

The photoconductivity signal is proportional to the number of free electrons in the conduction band.

Equilibrium between the electron trapping and thermal detrapping proceeds immediately upon exposure:

$$e_f + (\mathrm{T}) \leftrightarrow e_\mathrm{T}, \tag{2}$$

where (T) is an electron trap and e_T is an electron in the trap. The number of shallow traps and the initial number of free electrons can be estimated from signal intensity (I). Eq. (2) applies until all the free electrons disappear.

A shallow trapped electron may be converted into a deep trapped electron, and the photoconductivity signal falls accordingly:

$$e_\mathrm{T} \rightarrow e'_\mathrm{T}, \tag{3}$$

where e'_T is a trapped electron in a deep electron trap. This electronic process [Eq. (3)] appears as the fast component of decay (τ_1).

Some trapped electrons react with interstitial silver ions (Ag_i^+) at the deep traps and form silver atoms (Ag^0), after which the photoconductivity signal falls further:

$$e'_\mathrm{T} + Ag_i^+ \rightarrow Ag^0. \tag{4}$$

This ionic process [Eq. (4)] appears as the slow component of decay (τ_2). The repetition of these reciprocating electronic and ionic processes creates a latent image center.

At the same time, positive holes are trapped by hole traps to which the silver ion vacancy (V_{Ag}) subsequently gravitates, and a hole-complex ($[hV_{Ag}]$) is generated.

$$h + V_{Ag}^{-} \leftrightarrow [hV_{Ag}]. \quad (5)$$

The hole-complex diffuses and discharges as Br_2 at the crystal surface.

$$[hV_{Ag}] \rightarrow Br \rightarrow \tfrac{1}{2}Br_2. \quad (6)$$

At the same time, some trapped electrons react with the holes, and a recombination reaction renders these electrons extinct. The photoconductivity signal decreases with the decrease in the number of free electrons:

$$e'_T + h \rightarrow \text{recombination}. \quad (7)$$

This recombination reaction also appears as the slow component of decay (τ_2). When the recombination reaction occurs frequently, silver cluster (latent image center) formation becomes inefficient.

In our study, we made all microwave photoconductivity measurements at room temperature. It appears that the series of reactions occurs very quickly, so that separation of each reaction is difficult. While the τ_1 of this study apparently included τ_2, the ratio of τ_2 is unidentified. However, Eq. (3) is a trigger reaction of electron decay. So we tentatively assumed that the photoelectron lifetime of this study corresponds to the kinetics of the electronic process of Eq. (3).

Photoconductivity of Nanometer-Scale Silver Halide Emulsion

The ratio of surface area to volume of nanometer-scale silver halide crystals is greater than that of micrometer scale crystals. Because defects on the surface can act as shallow traps, there are many shallow traps on nanometer-scale crystals. It appears that a great number of free electrons are easily trapped [Eq. (2)], and signal decreases dramatically at the initial stage of decay. Thus, an optimum measurement condition to maximize the signal-to-noise ratio is necessary, just as it was in this study.

The signal of the pure silver halide system in Fig. 6(a) did not decay to the level preceding exposure (0 mV) but it decayed to about 60 mV. It may be that at the latter stage of decay a large number of free electrons are reintroduced as they escape from shallow traps [Eq. (2)]. Although there are many shallow traps on nanometer-scale crystals, latent image formation is inefficient.

The Effect of Adding RCOOAg

Because the light absorption[11] of silver halide at 355 nm is stronger than that of silver carboxylate, and because there was only a small amount (<10 mol %) of silver carboxylate in any of the RCOOAg-AgBrI admixtures, it may be presumed that the origin of the photoconductivity signals observed was the silver halide crystals.

The signal intensity on single exposure (Fig. 7, $n=1$) dropped with an increase in the ratio of silver carboxylate, suggesting that free electron population in the conduction band decreases as electron trapping and thermal detrapping seek equilibrium [Eq. (2)]. In general, free electrons (e_f) decrease as shallow traps (T) increase. This suggests that shallow traps increased with the addition of silver carboxylate.

Photoelectron lifetime after a single exposure (Fig. 8, $n=1$) decreased when silver carboxylate was present. The photoelectron lifetime reflects the relaxation process from shallow to deep traps [Eq. (3)]. It may be that the relaxation process with the shallow traps generated by the addition of silver carboxylate is different from the relaxation process involved with the intrinsic shallow traps of pure silver halide crystals.

In addition, while photoelectron lifetime changes in the presence of silver carboxylate, that change does not depend on the ratio of silver carboxylate present, suggesting that the photoelectron lifetime reflects the activity of each photoelectron on each individual shallow trap of the silver halide crystal.

As seen in Fig. 6(a), the level of signal convergence for all RCOOAg-AgBrI samples is about 20 mV, lower than the level for the pure silver halide crystal sample. Previously we reported that silver clusters form easily in a RCOOAg-AgBrI system, as indicated by diffuse reflectance spectrum measurement.[10] Therefore, it appears that the effect of adding silver carboxylate is to increase the number of shallow traps [Eq. (2)] and to promote electron decay through the generation of silver clusters [Eqs. (3) and (4)].

Analysis of Data From Repeated Exposures

In general, signal intensity falls with repeated exposures, which can be explained by the formation of silver clusters acting as electron traps.[11] In our previous report,[10] we found that silver clusters formed more efficiently in a RCOOAg-AgBrI admixture than in a pure AgBrI emulsion. As seen in Figure 7, the decrease in signal intensity after five exposures was greater than that after a single exposure for all samples. The decrease of the number of free electrons may be due to the formation of silver clusters that work as electron traps.

In the case of the pure AgBrI emulsion samples, neither signal intensity nor photoelectron lifetime showed appreciable change with the number of exposures (Figs. 7 and 8), perhaps because few silver atoms were formed even after five exposures. The formation of silver clusters (and thus latent image) is difficult to achieve with nanometer-scale silver halide crystals.

There are many reports[11] of a decrease in both signal intensity and photoelectron lifetime with an increase in the number of electron traps. However, Vekeman et al.[12] reported that signal intensity decreased but photoelectron lifetime increased with silver halide crystals doped with iridium. They explained that a trivalent iridium complex behaves chiefly as a transient electron trap, capturing photoelectrons during flash exposure and afterward releasing them thermally at room temperature. Furthermore, they reported that the hole capture cross section for a trivalent iridium complex was small. Consequently, the internal recombination step is quenched, and most iridium ions act as temporary electron traps.

In our previous report,[10] we found that whenever the number of exposures of the RCOOAg-AgBrI admixtures

increased, the maximum absorption of silver clusters in the vicinity of 500 nm increased, rather than shifting to a longer wavelength. This indicated that with each exposure the generation of new silver clusters proceeded more readily than the growth of existing silver clusters, suggesting that silver carboxylate enhances not the growth of existing clusters but the generation of new silver clusters.

We found photoelectron lifetimes to be prolonged (Fig. 8, $n=5$), indicating that the reaction process of Eq. (3) is retarded. In this case, the silver clusters that form after repeated exposures act as temporary electron traps, but, as with the trivalent iridium complexes referred to above,[13] the silver clusters do not promote the relaxation process.

Finally, photoelectron lifetime showed little change with increasing concentration of silver carboxylate (Fig. 8), suggesting that photoelectron decay is not strongly dependent on the density of silver carboxylate. Photoelectron decay may involve both silver carboxylate and silver halide crystals. It appears that the lattice relaxation process occurs only at traps comprised of silver carboxylate on the surfaces of the silver halide crystals.

The Identity of Shallow Traps After One Exposure

Figure 7 shows signal intensities falling with the addition of silver carboxylate, indicating that the presence of silver carboxylate brings about an increase in shallow traps. The appearance of these traps is somehow due to the silver carboxylate present.

Yamane et al.[4] has reported silver halide emulsions (pAg=8.3) with silver carboxylate in water media exhibiting photographic performance similar to a low pAg emulsion (pAg=4). In an earlier report,[10] we found that the pAg of a silver halide emulsion decreased with silver carboxylate concentration, i.e., free silver ion concentration increased from dissociation of the silver carboxylate.

Usanov et al. reported that photosensitive silver halides and silver carboxylate can be co-precipitated. Alternatively, silver carboxylate ions can be completely converted to silver halide, and can be added back to silver carboxylate.[13,14]

In this study, we intended to avoid creating epitaxial interfaces between the silver carboxylate and the silver halide crystals. However, it is quite possible that dissociated silver carboxylate re-precipitated on the surfaces of silver halide during coating and drying. Such re-precipitated silver carboxylate might adsorb as a single molecule or adsorb as an aggregate; just how the silver carboxylate adsorbs is unclear. However, it appears that the process results in many shallow traps comprised of silver carboxylate on the surfaces of silver halide crystals.

CONCLUSIONS

Microwave photoconductivity measurements revealed that the silver cluster formation process upon exposure of a RCOOAg-AgBrI admixture differs from that process when a pure AgBrI emulsion is exposed. The number of shallow electron traps increased when silver carboxylate was present in silver halide crystal emulsions. This increased number of shallow electron traps enabled a lattice relaxation process, thus promoting the formation of silver clusters. We conclude that silver carboxylate greatly affects latent image formation in silver salt photothermographic materials.

REFERENCES

[1] R. Cowdery-Corvan and D. R. Whitcomb, in *Handbook of Imaging Materials*, edited by A. S. Diamond and D. S. Weiss (Marcel Dekker, New York, 2002), p. 473.

[2] (a) C. F. Zou, M. R. V. Sahyun, B. Levy, and N. Serpone, J. Imaging Sci. Technol. **40**, 94 (1996); (b) A. von König, H. Kampfer, E. M. Brinckmann, and F. C. Heugebaert, "Photographic light-sensitive and heat developable material", U.S. Patent 3,933,507 (1976); (c) J. W. Shepard, J. Appl. Photogr. Eng. **8**, 210 (1982); (d) B. Levy, Photograph. Sci. Eng. **27**, 204 (1983).

[3] (a) P. L. Potapov, D. Schryvers, H. Strijckers, and C. Van Roost, J. Imaging Sci. Technol. **47**, 115 (2003); (b) H. L. Strijckers, J. Imaging Sci. Technol. **47**, 100 (2003).

[4] K. Yamane and S. Yamashita, (a) *Proc. ICIS'02* (SPSTJ, Tokyo, 2002), p. 29; (b) *Annual Conference of Soc. Photogr. Sci. Technol.* (SPSTJ, Tokyo, 2005), p. 14.

[5] S. M. Ho Kimura, T. Mitsuhashi, K. Kuge, and A. Hasegawa, *2005 Beijing International Conference on Imaging: Technology and Applications for the 21st Century* (CSIST and IS&T, Beijing, 2005), p. 60.

[6] J. Beutel, Photograph. Sci. Eng. **19**, 95 (1975); J. Appl. Phys. **46**, 4649 (1975).

[7] T. Harada, T. Iijima, and T. Koitabashi, Photograph. Sci. Eng. **26**, 137 (1982).

[8] R. J. Deri, J. P. Spoonhower, and J. F. Hamilton, J. Appl. Phys. **57**, 1968 (1985).

[9] L. M. Kellogg, N. B. Liebert, and T. H. James, Photograph. Sci. Eng., **16**, 115 (1972).

[10] S. M. Ho Kimura, T. Suzuki, T. Mitsuhashi, K. Kuge, and A. Hasegawa, J. Soc. Photogr. Sci. Technol. Jpn. **68**, 197 (2006).

[11] (a) L. M. Kellogg, Photograph. Sci. Eng. **18**, 378 (1974); (b) S. S. Collier, Photograph. Sci. Eng. **20**, 43 (1976); (c) A. Hasegawa, T. Kumazumi, K. Iion, and T. Sakaguchi, J. Soc. Photogr. Sci. Technol. Jpn. **50**, 470 (1987); (d) K. Kuge, H. Shimabukuro, T. Tsutsumi, M. Kato, K. Sakashita, H. Kumagai, N. Aoki, A. Hasegawa, and N. Mii, Imaging Sci. J. **48**, 107 (2000).

[12] G. Vekeman, Y. B. Peng, W. Maenhout-Van der Vorst, and F. Cardon, J. Imaging Sci. **32**, 187 (1988).

[13] Yu. E. Usanov and T. B. Kolesova; (a) J. Imaging Sci. Technol. **40**, 104 (1996); (b) *Proc. ICIS1998* (KVCV, Antwerp, Belgium, 1998), p. 67.

[14] B. B. Bokhonov, L. P. Burleva, D. R. Whitcomb, N. C. Howlader, and L. M. Leichter; (a) U.S. Patent 6,803,177 (2004); (b) U.S. Patent 7,060,426 (2007).